

# Toughening of a brittle thermosetting polymer: Effects of reinforcement particle size and volume fraction

R. P. SINGH\*, M. ZHANG, D. CHAN

*Mechanics of Advanced Materials Laboratory, Department of Mechanical Engineering, State University of New York, Stony Brook, NY 11794-2300, USA*

*E-mail: raman.singh@sunsyb.edu*

Micron- and nanometer-sized aluminum particles were used as reinforcements to enhance the fracture toughness of a highly-crosslinked, nominally brittle, thermosetting unsaturated polyester resin. Both particle size and particle volume fraction were systematically varied to investigate their effects on the fracture behavior and the fracture toughness. It was observed that, in general, the overall fracture toughness increased monotonically with the volume fraction of aluminum particles, for a given particle size, provided particle dispersion and deagglomeration was maintained. The fracture toughness of the composite was also strongly influenced by the size of the reinforcement particles. Smaller particles led to a greater increase in fracture toughness for a given particle volume fraction. Scanning electron microscopy of the fracture surfaces was employed to establish crack front trapping as the primary extrinsic toughening mechanism. Finally, the effects of particle volume fraction and size on the tensile properties of the polyester-aluminum composite were also investigated. The measured elastic modulus was in accordance with the rule-of-mixtures. Meanwhile, the tensile strength was slightly reduced upon the inclusion of aluminum particles in the polyester matrix. © 2002 Kluwer Academic Publishers

## 1. Introduction

Highly cross-linked thermosetting polymers, such as epoxy resins and unsaturated polyesters, are an important class of synthetic materials. Their main distinction from other types of polymers lies in their densely cross-linked molecular structure. This cross-linking leads to a number of superior properties including high glass transition temperatures, high modulus and specific strength, high creep resistance, good dimensional stability at elevated temperature, and good solvent resistance. These properties in conjunction with ease of processing have led to the extensive use of thermosetting polymers as adhesives, potting and encapsulating materials, tooling compounds, electronic substrates and packaging, and perhaps most importantly as matrix materials for reinforced composites.

Unfortunately, the high degree of molecular cross-linking in thermosetting polymers also makes them inherently brittle with poor resistance to crack initiation and propagation. This lack of toughness severely impacts the performance of highly cross-linked thermosets in almost all applications. For example, *it is the lack of matrix toughness that governs two out of the three primary damage initiation modes in fiber-reinforced laminated composites, viz. matrix cracking and delamination.* Thus, improving the fracture tough-

ness of thermosetting polymers will lead to significantly enhanced performance when used as is, and will also enhance the damage initiation threshold and long-term reliability of fiber-reinforced composites.

Improving the fracture toughness of thermosetting resins has been the subject of considerable research. Typically, these approaches have involved the addition of micron-sized soft (elastomeric or thermoplastic) or rigid (glass or ceramic) particles into the polymer matrix. These filler particles are then expected to provide extrinsic toughening mechanisms.

In the first approach, micron-sized rubber particles are dispersed in the polymer matrix to enhance the overall fracture toughness by triggering localized shear yielding of the polymer [1–6]. However, highly cross-linked thermosetting polymers are incapable of extensive shear yielding. Thus, the effectiveness of rubber additions decreases rapidly with increasing cross-link density [7, 8]. Moreover, the addition of rubber introduces other deleterious effects, such as a reduction in the elastic modulus and tensile strength, decreased creep resistance, poor hot/wet performance, and a lowering of the glass transition temperature. Alternatively, ductile thermoplastic particles may be dispersed in the thermosetting polymer to provide extrinsic mechanisms for increasing the overall toughness [9–12].

\* Author to whom all correspondence should be addressed.

However, only moderate increases in the fracture toughness have been observed, especially for low volume fractions of added thermoplastic particles [12]. Other mechanical properties such as elastic modulus and high temperature performance are often compromised. Investigators have also explored the incorporation of high modulus ceramic and glass particles into the polymer matrix [13–15]. These particles generally improve the elastic modulus and the glass transition temperature, but the increase in fracture toughness is usually only moderate, especially at low volume fractions of added particles [16]. Also, the high density of inorganic particles makes uniform mixing and even dispersion difficult at low volume fractions.

Thus it is apparent that the conventional approach of introducing micron-sized particles into the polymer matrix has failed to yield significant improvements in the fracture toughness of highly cross-linked thermosetting polymers. Furthermore, other mechanical properties are often compromised, or there are processing problems. However, recent research indicates that the dispersion of sub-micrometer and nanometer sized inorganic particles presents a novel approach towards improving the mechanical properties of polymers. Such materials, which include polymer nanocomposites, have the potential for significantly enhanced and unique properties as compared to polymers reinforced with conventional microscale fillers [17].

Several researchers have investigated nanoscale reinforcement of both thermoplastic and thermosetting polymers. These reinforcements are formed either as inorganic-organic hybrids [18, 19], or as intercalated/exfoliated polymer-silicate structures [20–22]. These materials can exhibit substantial enhancements in the modulus, yield strength and heat resistance of the polymer. While these studies have not focussed on fracture toughness as the primary issue, there are clear indications that reducing the size of reinforcement particles could lead to significant improvements in fracture toughness and resistance to crack growth. Nevertheless, despite these observations there is limited fundamental information regarding the effects of reinforcement size on fracture processes, toughening mechanisms and the resulting overall fracture toughness.

This paper addresses this issue and presents a systematic characterization of the fracture behavior of a highly cross-linked thermosetting polymer reinforced with high-modulus inorganic particles, as a function of particle size and particle volume fraction. Such an understanding would then be essential for identifying parameters that will lead to the design and fabrication of optimally toughened thermosetting polymers.

## 2. Fabrication of composite materials

### 2.1. Selection of composite material constituents

The material system investigated consisted of unsaturated polyester reinforced with varying volume fractions of micrometer and nanometer sized aluminum particles. Details of the MR 10790 unsaturated polyester resin [23] are listed in Table I. This resin represents a typical highly cross-linked thermosetting polymer that exhibits brittle failure. Fur-

TABLE I Properties and curing methodology of the MR 10790 unsaturated polyester resin

Polymer	MR 10790 polyester resin (Ashland Chemical)
Curing agents	Methyl ethyl ketone peroxide (0.85% by weight) Cobalt octoate (0.03% by weight)
Curing cycle	48 hrs at 25°C; 4 hrs at 52°C; 5 hrs at 63°C
Young's modulus	3.25 GPa
Fracture toughness	0.64 MPa · m <sup>1/2</sup>
Density	1160 kg/m <sup>3</sup>

TABLE II Properties of the various aluminum particles used as reinforcement

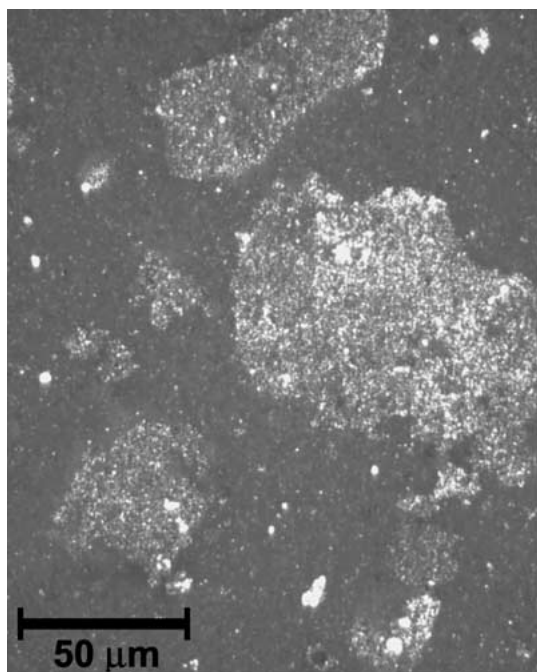
Property	Aluminum A	Aluminum B	Aluminum C
Nominal average diameter	20 μm	3.5 μm	100 nm
Diameter range	17–23 μm	3–4.5 μm	100 nm
Young's modulus	70 GPa	70 GPa	70 GPa
Fracture toughness	30 MPa · m <sup>1/2</sup>	30 MPa · m <sup>1/2</sup>	30 MPa · m <sup>1/2</sup>
Density	2699 kg/m <sup>3</sup>	2699 kg/m <sup>3</sup>	2699 kg/m <sup>3</sup>

thermore, this polyester has numerous applications as laminated composites; tooling, casting, and molding compounds; construction, electrical and aerospace adhesives and electrical encapsulations [23]. Aluminum particles were selected as the reinforcement phase based on two factors: consistency in intrinsic particle modulus, and availability of particles in various sizes. The use of metal particles ensures that intrinsic toughness and modulus are independent of particle size. In the case of ceramic and glass particles, the internal defect size and hence the intrinsic particle strength is a function of particle size. Aluminum was chosen specifically because it was readily available as both micrometer and nanometer sized particles. As listed in Table II, three nominal particle sizes were employed: 20 μm, 3.5 μm and 100 nm. This represented a greater than two orders-of-magnitude variation in particle size.

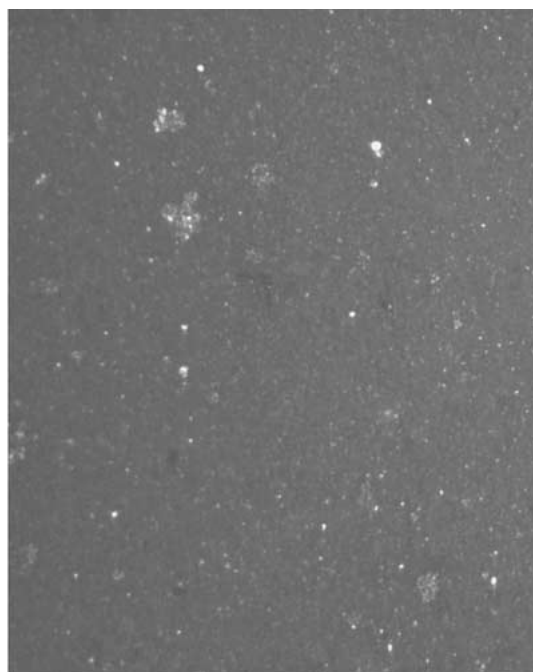
### 2.2. Casting of polyester-aluminum composites

Composite materials were fabricated by incorporating the three types of aluminum particles in the polyester resin at different volume fractions. Reinforcement quantities of interest were 1%, 2%, 5% and 10% of the particles by weight, which resulted in volume fractions of 0.5%, 0.9%, 2.3% and 4.4%, respectively. The use of a direct mixing approach for fabricating these composites provides flexibility in exercising independent control over reinforcement material, reinforcement geometry (size, morphology and size distribution) and interfacial conditions.

The aluminum particles were added to the liquid polyester resin and mechanical blending was employed to uniformly mix and disperse the particles. This liquid resin-particle mixture then was degassed under vacuum to remove air bubbles trapped during the blending process. After degassing, appropriate amounts of the curing agent, methylethylketoneperoxide (MEKP), and accelerator, cobalt octoate, were blended into the liquid mixture. After uniform mixing, the mixture was briefly degassed once again before being poured into pre-prepared molds for casting.



(a) Without ultrasonic disruption.



(b) With ultrasonic disruption.

Figure 1 Effect of ultrasonic disruption on particle dispersion and deagglomeration.

The molds were allowed to stand at room temperature for 48 hours. This resulted in cast sheets that were tack free and could be handled easily. These sheets were released from the molds and subjected to a specific elevated temperature curing cycle (52°C for 4 hours followed by 63°C for 5 hours) to complete the curing process. This process resulted in complete cross-linking of the unsaturated polyester resin with minimal residual stresses.

An additional step was required to ensure even dispersion and deagglomeration of the 100 nm particles. In this case, ultrasonic disruption was employed after mechanical blending to minimize particle agglomeration. The ultrasonic transducer was operated in a fixed amplitude and cyclic disruption mode to maximize deagglomeration, while minimizing the modification of the liquid polyester resin. Optical micrography of polished cross-sections was carried out to ensure the effectiveness of ultrasonic disruption in particle deagglomeration and dispersion. Fig. 1 shows that the use of this procedure greatly reduced the formation of large agglomerates.

At the same time, it was also necessary to ensure that ultrasonic disruption did not change the molecular structure of the neat polyester resin and affect its mechanical properties. Experiments were carried out to quantify the quasi-static fracture toughness of cured unsaturated polyester (neat - with no reinforcement) with and without exposure to ultrasonic disruption. The fracture toughness of the polyester resin did not change after extensive exposure to ultrasonic disruption. This was taken as evidence that the molecular structure was unaffected.

### 2.3. Fabrication of specimens

Three-point-bend single-edge-notched (3PB-SEN) fracture specimens were machined from the cast

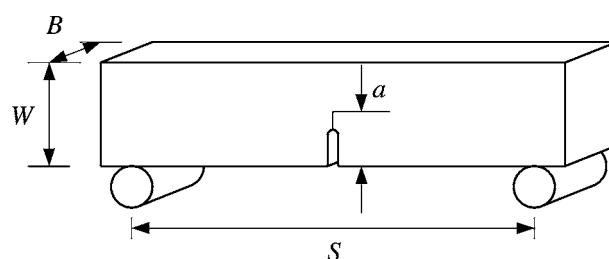


Figure 2 Schematic of the single-edge-notched specimen for three-point-bend fracture testing.

polyester sheets for testing. The specimens had a nominal length,  $L$ , of 55.9 mm, a height,  $W$ , of 12.7 mm and a thickness,  $B$ , of 6.35 mm, as shown in Fig. 2. A 4.25 mm deep notch was first cut into the center of the specimen using a diamond saw. A fresh razor blade was then tapped into the cut with a hammer to create a naturally sharp crack. The actual length of the overall crack,  $a$ , was measured after the fracture experiment by observation in an optical microscope equipped with a micrometer stage. All the specimens used for valid fracture tests had a nominal crack length to specimen width ratio,  $a/W$ , of  $\sim 0.5$ , as per ASTM standard 5045 [24].

## 3. Testing and characterization of polyester-aluminum composites

### 3.1. Determination of fracture toughness

The quasi-static fracture toughness of the polyester-aluminum composites was measured as a function of particle size and particle volume fraction. Single-edge-notched fracture specimens were loaded quasi-statically under three-point-bending until the initiation of fracture. The specimens were loaded in a displacement-controlled mode and the crosshead speed

was fixed at 5 mm/minute to keep the loading rate constant. The maximum applied load at the point of failure was measured using a 500 N load-cell and then used to quantify the quasi-static fracture toughness of the composite being tested.

The mode-I stress intensity factor was determined from these measurements as per Equation 1 [25],

$$K_Q = \frac{3S\sqrt{a}}{2BW^2} Y\left(\frac{a}{W}\right) F_{\max} \quad (1)$$

where,  $F_{\max}$  is the force required for fracture,  $B$  is the specimen thickness,  $W$  is the specimen width,  $S$  is the span,  $a$  is the crack length and  $Y$  is a geometry factor given as [26],

$$Y\left(\frac{a}{w}\right) = \frac{1.99 - \frac{a}{w}\left(1 - \frac{a}{w}\right)\left[2.15 - 3.93\frac{a}{w} + 2.7\left(\frac{a}{w}\right)^2\right]}{\left(1 - 2\frac{a}{w}\right)\left(1 - \frac{a}{w}\right)^{3/2}} \quad (2)$$

Using this experimental procedure the composite fracture toughness was determined as a function of volume fraction of aluminum particles for each of the three particle sizes. Multiple experiments were conducted (at least 5) for each material combination to establish the statistical spread of experimental data with reasonable confidence. This is denoted by error bars in the plots of experimental data.

Fig. 3 shows the variation of composite fracture toughness as a function of the volume fraction of 20  $\mu\text{m}$ , 3.5  $\mu\text{m}$ , and 100 nm aluminum particles added to the polyester resin. For the case of 20  $\mu\text{m}$  particles the fracture toughness of the polyester-aluminum composite increased monotonically with the volume fraction of aluminum particles. For an 4.4% volume fraction of reinforcement particles the fracture toughness increased by 22%, as compared to the unreinforced polyester. A similar trend was observed for reinforcement by 3.5  $\mu\text{m}$  aluminum particles and the fracture toughness

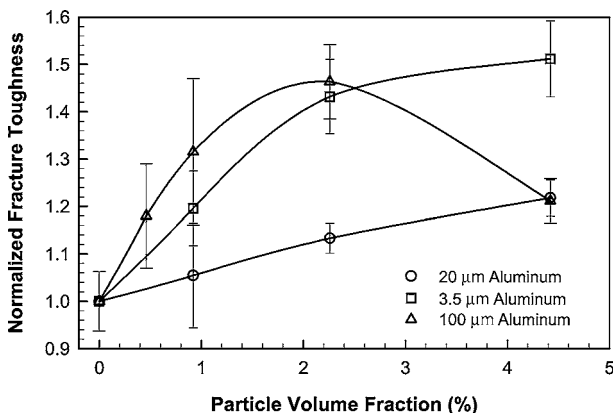


Figure 3 Variation of fracture toughness as a function of volume fraction for reinforcement by 20  $\mu\text{m}$ , 3.5  $\mu\text{m}$  and 100 nm aluminum particles.

increased monotonically with the volume fraction of aluminum particles. However, the relative increase in fracture toughness was significantly greater for reinforcement by 3.5  $\mu\text{m}$  particles as compared to that observed for reinforcement by 20  $\mu\text{m}$  particles. For reinforcement by 4.4% volume fraction of 3.5  $\mu\text{m}$  aluminum particles the fracture toughness increased by 51%, which is more than twice the increase observed using 20  $\mu\text{m}$  particles. When the size of the reinforcement aluminum particles was further decreased to 100 nm a different trend was observed, as shown in Fig. 3. For this case the fracture toughness increased rapidly till a particle volume fraction of 2.3%. As the particle volume fraction was increased further the fracture toughness registered a sharp decrease. Thus, from Fig. 3 it is evident that fracture toughness is strongly governed by the size of the reinforcement particles. Smaller particles lead to a greater increase in the overall fracture toughness for a given volume fraction. This trend is not observed only for the case of reinforcement by 100 nm aluminum particles in volume fractions greater than 2.3%.

### 3.2. Fracture processes and mechanisms governing toughness

The addition of tough reinforcement particles in highly cross-linked brittle polymers can give rise to several extrinsic mechanisms that govern the increase in overall fracture toughness. These mechanisms include crack trapping, crack-face bridging, crack-path deflection and crack-tip shielding by microcracking. Microscopic observations of the fracture surfaces were carried out using scanning electron microscopy (SEM) to characterize the interaction of the crack with the reinforcing particles and to identify the extrinsic toughening mechanisms.

Fig. 4 shows an SEM micrograph of the fracture surface for polyester reinforced with 20  $\mu\text{m}$  aluminum particles. The fracture surface showed the formation of steps, or 'fracture tails' that emanate from the reinforcing particles along the direction of crack growth. These fracture steps were the result of the aluminum particles impeding the growth of the crack in the polyester matrix, which led to crack front trapping [27]. Besides the formation of these steps, the fracture surface was fairly flat, which indicates that crack path deflection did not occur. Moreover, the aluminum particles appeared to be debonded from the polyester matrix and did not show any evidence of particle yielding and deformation. Thus, extensive crack face bridging did not occur either. Finally, microcracking of the polyester matrix was also not observed. In this manner, crack front trapping was established to be the primary extrinsic mechanism responsible for the increase in fracture toughness of polyester reinforced with 20  $\mu\text{m}$  aluminum particles. These observations were made for all the particle volume fractions that were investigated. Similar observations were made using scanning electron microscopy of the fracture surface of polyester reinforced with 3.5  $\mu\text{m}$  particles, as shown in Fig. 5. This micrograph also shows the formation of steps in the fracture

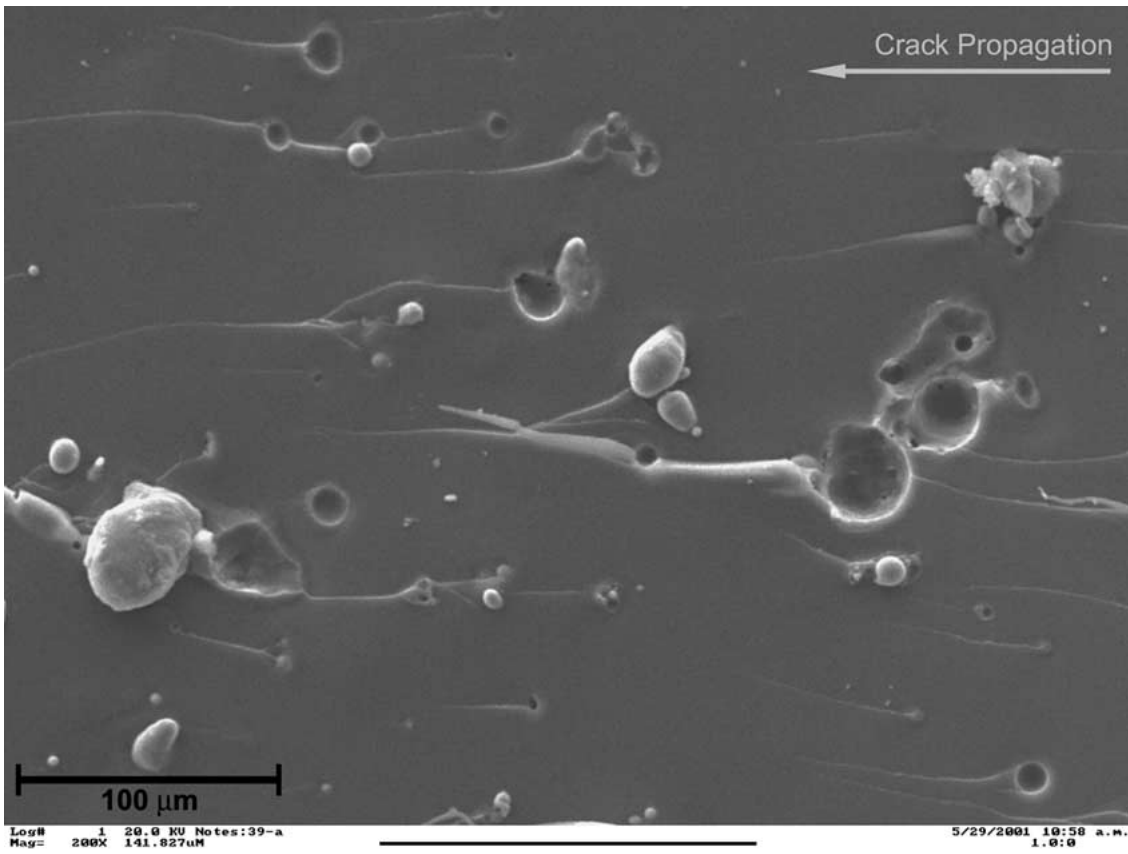


Figure 4 SEM micrograph of the fracture surface of polyester resin reinforced with 20  $\mu\text{m}$  aluminum particles.

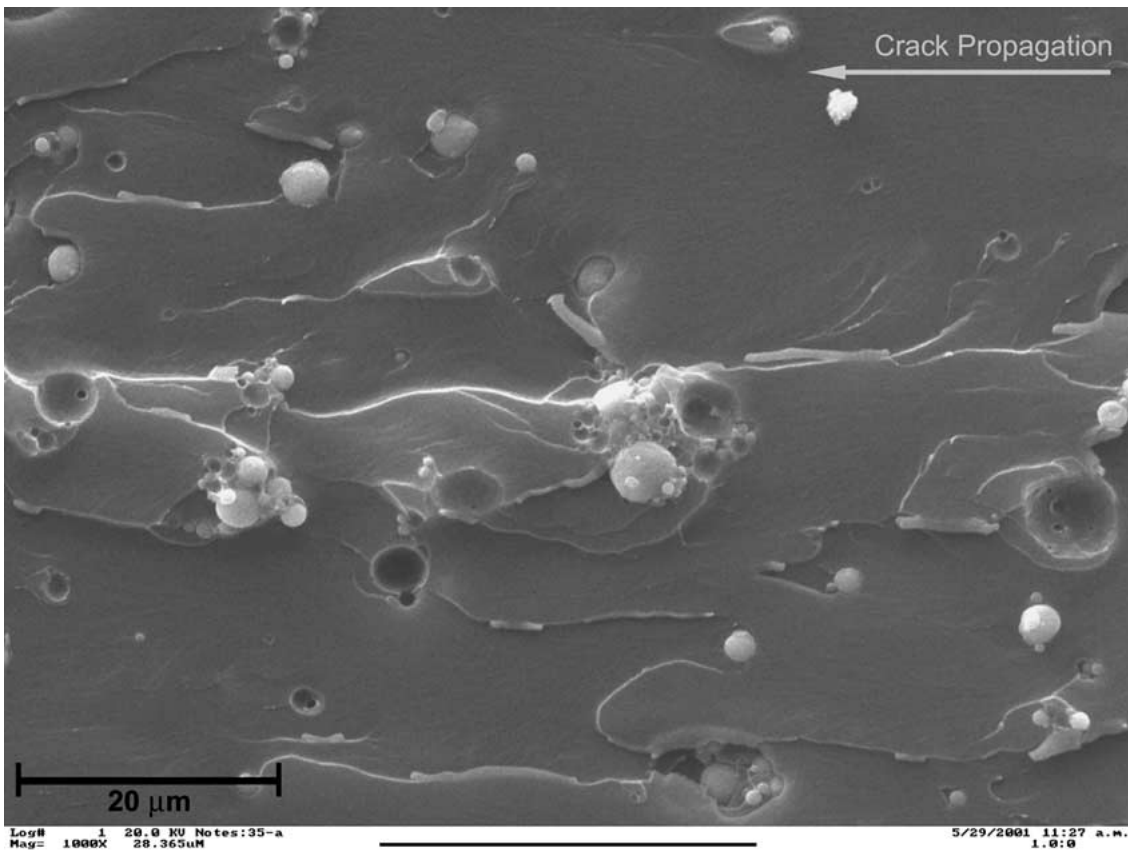


Figure 5 SEM micrograph of the fracture surface of polyester resin reinforced with 3.5  $\mu\text{m}$  aluminum particles.

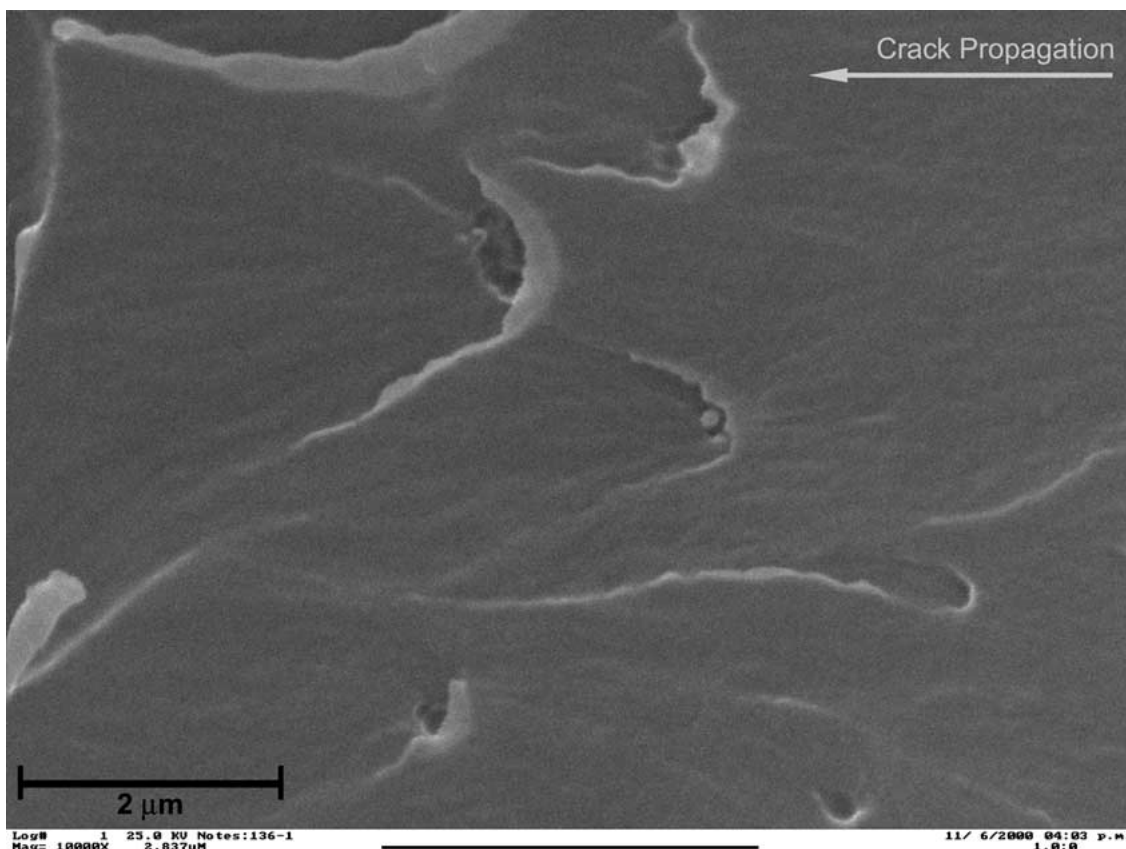


Figure 6 SEM micrograph of the fracture surface of polyester resin reinforced with 100 nm aluminum particles.

surface emanating from the aluminum particles in the direction of crack growth, which established crack front trapping. No evidence of crack path deflection, crack face bridging, or microcracking was observed. Thus, crack front trapping was once again identified as the primary toughening mechanism for the 3.5  $\mu\text{m}$  aluminum particles for all volume fractions investigated.

However, for the case of reinforcement by 100 nm aluminum particles the fracture mechanisms were found to be dependent on the particle volume fraction. For the case of low volume fractions ( $\leq 2.3\%$ ) the particles were uniformly distributed and contributed to crack front trapping, as shown in Fig. 6. The fracture surface exhibited features similar to those observed for the case of 20  $\mu\text{m}$  and 3.5  $\mu\text{m}$  aluminum particles. In contrast, when the particle volume fraction was greater than 2.3%, the fracture surface exhibited marked differences, as shown in Fig. 7. In such a case, the aluminum particles tended to clump together and form agglomerates. These particle clusters inhibited proper wet-out, promoted the trapping of air and led to the formation of voided spaces that acted as damage initiation sites. As a result, the fracture surface appeared to be 'flaky' and no evidence of crack trapping was observed.

These observations of the fracture surfaces for reinforcement with 100 nm aluminum particles are consistent with the quantitative measurements of fracture toughness presented earlier (in Fig. 3). For low volume fractions ( $\leq 2.3\%$ ), the particles were well-distributed and promoted crack front trapping, which led to an increase in overall fracture toughness. However, at volume fractions greater than 2.3% the particles tended to

agglomerate and were unable to promote crack trapping. Thus, the reinforcement particles were unable to provide the primary extrinsic toughening mechanisms and there was a decrease in the value of the fracture toughness, as depicted in Fig. 3.

The formation of these small agglomerates, at volume fractions greater than 2.3%, occurred despite the use of ultrasonic disruption. Ultrasonic disruption was found to be very effective in preventing the formation of large agglomerates, as discussed earlier. However, alternate chemical and/or mechanical treatments would be required to further disperse and deagglomerate 100 nm particles at volume fractions greater than 2.3%. The experimental observations also imply that improvements in particle dispersion would then lead to even greater enhancements in the overall fracture toughness.

### 3.3. Variation of elastic modulus and tensile strength

Experiments were also conducted to determine material response under uniaxial tension. Dogbone shaped specimens were subjected to uniaxial loading to the point of failure. The applied load was measured by a 2500 N load cell, and longitudinal strain was monitored using a strain gage mounted in the center of the specimen. These experimental measurements were then used to determine the elastic modulus and tensile failure strength of the polyester-aluminum composite material.

The experimental results indicate that the elastic modulus of the polyester-aluminum composite was not affected by the reinforcement particle size. However,

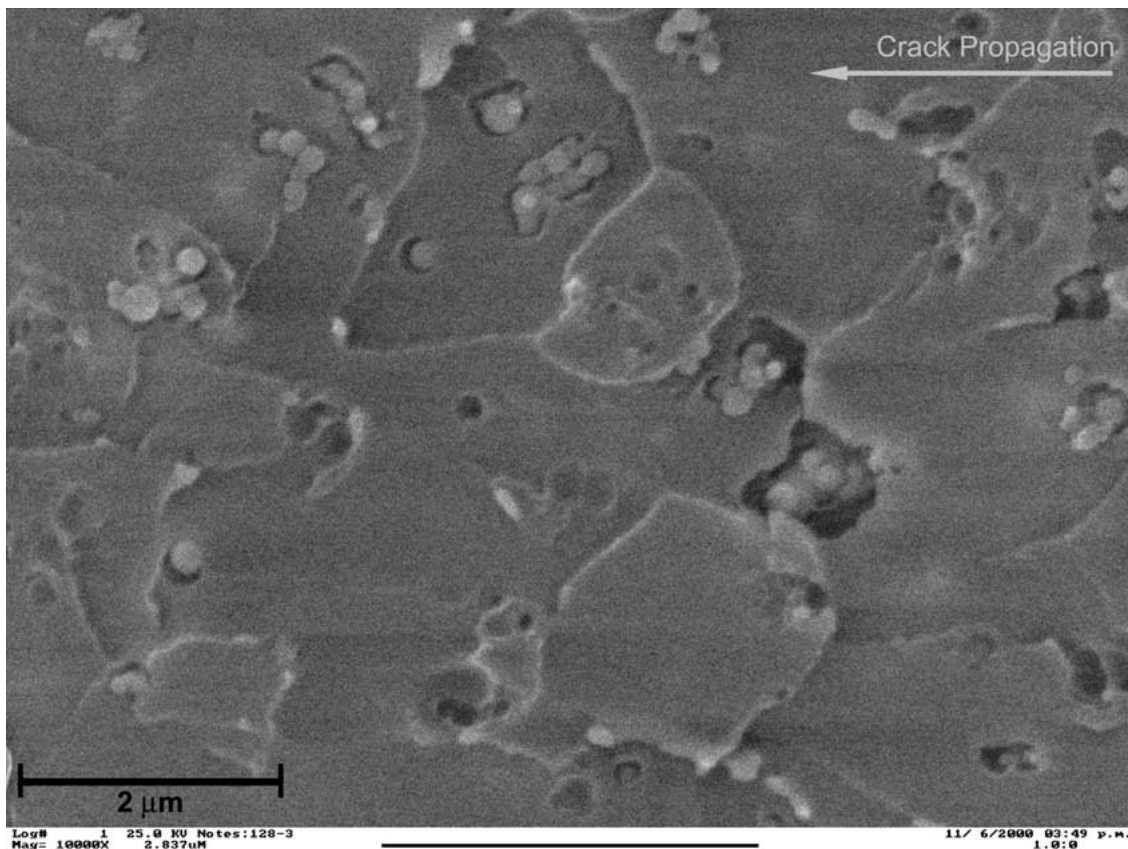


Figure 7 SEM micrograph of the fracture surface of polyester resin reinforced with 100 nm aluminum particles showing agglomeration.

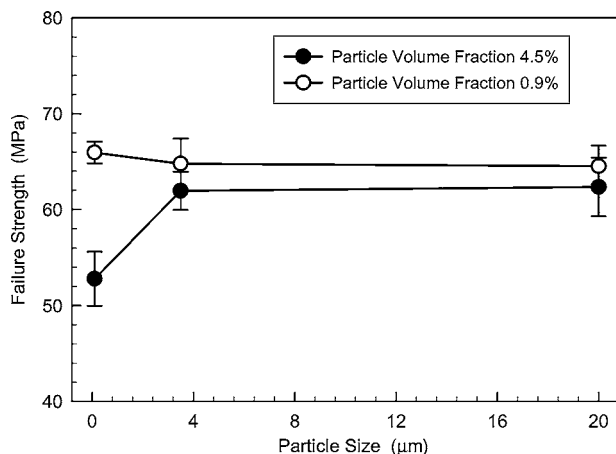


Figure 8 Variation of tensile failure strength of polyester-aluminum composites as a function of particle size and volume fraction.

there was a nominal dependence of the modulus on the volume fraction of aluminum particles in accordance with the “rule-of-mixtures”,

$$E_c = \varphi_m E_m + \varphi_p E_p \quad (3)$$

where  $E_c$ ,  $E_m$ , and  $E_p$  are elastic moduli of the composite, polyester matrix and aluminum particles, respectively, and  $\varphi_m$  and  $\varphi_p$  are volume fraction of polyester matrix and aluminum particles, respectively.

Fig. 8 shows the variation in tensile strength as a function of reinforcement particle size and particle volume fraction. There was a slight degradation in the tensile strength as the volume fraction of the aluminum particles was increased. This is because the particles

debonded from the polyester matrix during the tensile loading process prior to final failure. Thus, at the point of failure the load was borne primarily by the polyester matrix and the debonded aluminum particles formed potential damage initiation sites. In that case, a greater volume fraction of particles implied a reduction in tensile strength. On the other hand, particle size did not have any influence on the tensile strength, for a given particle volume fraction. The only exception to this observation was the case of 100 nm particles added in volume fractions greater than 2.3%. The sharp decrease in the tensile strength that was observed for this material combination was due to particle agglomeration, as discussed earlier.

#### 4. Conclusions

This investigation was focussed on the toughening of highly cross-linked thermosetting unsaturated polyester by the incorporation of micron- and nanometer-sized aluminum particles. The effects of reinforcement particle size and particle volume fraction on the overall toughness and fracture behavior of polyester-aluminum composites was investigated by systematically varying the size (20 μm, 3.5 μm, 100 nm) and volume fraction (0.5%, 0.9%, 2.3% and 4.4%) of the aluminum particles. From experimental observations it was established that the enhancement of fracture toughness is strongly influenced by both these parameters. In general the fracture toughness increased monotonically with the volume fraction of aluminum particles, for a given particle size. Furthermore, it was observed that the increase in fracture toughness was

significantly greater for smaller particles, for a given particle volume fraction.

Crack front trapping was established as the primary extrinsic toughening mechanism by conducting scanning electron microscopy of the fracture surfaces. It was observed that it is essential to maintain uniform particle dispersion and deagglomeration, and proper particle wet-out in order to ensure that the reinforcement particle promote crack trapping. While ultrasonic disruption was found to be very effective in preventing the formation of large agglomerates, it was determined that further chemical and/or mechanical treatment would be required to disperse and deagglomerate 100 nm aluminum particles at greater volume fractions.

Finally, the effects of particle volume fraction and size on the tensile properties of the polyester-aluminum composite were also investigated. The measured elastic modulus was in accordance with the rule-of-mixtures. Meanwhile, the tensile strength was slightly reduced upon the inclusion of aluminum particles in the polyester matrix.

## References

1. J. N. SULTAN and F. J. MCGARRY, *Polymer Engineering and Science* **13** (1973) 29.
2. T. T. WANG and H. M. J. ZUPKO, *J. Appl. Polym. Sci.* **26** (1981) 2391.
3. A. J. KINLOCH, S. J. SHAW, D. A. TOD and D. L. HUNSTON, *Polymer* **24** (1983) 1341.
4. G. A. CROSBIE and M. G. PHILLIPS, *J. Mater. Sci.* **20** (1985) 182.
5. A. F. YEE and R. A. PEARSON, *ibid.* **21** (1986) 2462.
6. J. S. ULLETT and R. P. CHARTOFF, *Polymer Engineering and Science* **35** (1995) 1086.
7. R. A. PEARSON and A. F. YEE, *J. Mater. Sci.* **24** (1989) 2571.
8. J. F. HWANG, J. A. MANSON, R. W. HERTZBERG, G. A. MILLER and L. H. SPERLING, *Polymer Engineering Science* **29** (1989) 1466.
9. C. B. BUCKNALL and I. K. PARTRIDGE, *Polymer* **24** (1983) 639.
10. A. J. KINLOCH, M. L. YUEN and S. D. JENKINS, *J. Mater. Sci.* **29** (1994) 3781.
11. J. H. HODGKIN, G. P. SIMON and R. J. VARLEY, *Polymers For Advanced Technologies* **9** (1998) 3.
12. R. A. PEARSON, *Advances in Chemistry Series* Vol. 233 (1993) 405.
13. J. SPANOUDAKIS and R. J. YOUNG, *J. Mater. Sci.* **19** (1984) 473.
14. A. MOLONEY, H. H. KAUSCH and H. R. STIEGER, *ibid.* **19** (1984) 1125.
15. M. HUSSAIN, A. NAKAHIRA, S. NISHIJIMA and K. NIIHARA, *Materials Letters* **27** (1996) 21.
16. A. G. EVANS, S. WILLIAMS and P. W. R. BEAUMONT, *J. Mater. Sci.* **20** (1985) 3668.
17. H. GLEITER, *Acta Materialia* **48** (2000) 1.
18. B. M. NOVAK, *Advanced Materials* **5** (1993) 422.
19. J. E. MARK, *Polymer Engineering and Science* **36** (1996) 2905.
20. A. OKADA, M. KAWASUMI, T. KURAUCHI and O. KAMIGAITO, *Abstracts of Papers of The American Chemical Society* **194** (1987).
21. E. P. GIANNELIS, *Applied Organometallic Chemistry* **12** (1011) (1998) 675.
22. P. C. LEBARON, Z. WANG and T. J. PINNAVAIA, *Applied Clay Science* **15**(12) (1999) 11.
23. Ashland Specialty Chemical Company, 5200 Blazer Parkway, Dublin, OH 43017, USA.
24. American Society of Testing and Materials, "Standard Test Methods for Plane-Strain Fracture Toughness and Strain Energy Release Rate of Plastic Materials," Annual Book of ASTM Standards, Designation D5045-99, 1999.
25. T. L. ANDERSON, "Fracture Mechanics: Fundamentals and Applications" (CRC Press, Boca Raton, FL, 1991).
26. J. E. SRAWLEY, *International Journal of Fracture* **12** (1976) 475.
27. F. F. LANGE, *Phil. Magazine* **22** (1970) 983.

Received 16 January  
and accepted 28 August 2001